POWER CONVERTER FOR FAULT TOLERANT SEGMENTED PEMFC AND ASSOCIATED TECHNOLOGY

A. De Bernardinis[1,*], O. Béthoux[2], E. Frappé[1]
[1]IFSTTAR LTN, 25 Allée des Marronniers, 78000 Versailles, France
[2] LGEP Cnrs UMR 8507, SUPELEC, 11 rue Joliot Curie, 91192 Gif-sur-Yvette, France
alexandre.de-bernardinis@ifsttar.fr; olivier.bethoux@lgep.supelec.fr; emmanuel.frappe@gmail.com

Keywords : PEMFC, Fault tolerance, Power converter, Segmentation, Technology

ABSTRACT
In the context of power increase for transport applications or on-board auxiliaries systems, long fuel cell stacks may be subject to disparities (fluidics, temperature) and can be the cause of possible failures. Fuel cell electric power is conditioned by a power converter. This latter, combined with a fault detection strategy, can also act to manage the fault. This work deals with power converter topologies dedicated to a segmented high power fuel cell. The considered fuel cell generator is a 30kW 3-part segmented Polymer Electrolyte Membrane Fuel Cell. Each fuel cell segment of 10kW can be controlled independently from an electrical point of view according to its state-of-health. The converter topology has to be compact, reliable and energy efficient. The resonant isolated boost as converter "technology brick", allowing soft switching over a large operating range, is a candidate topology. A pre-prototype converter is designed fulfilling high efficiency and integration objectives using recent silicon technology MOSFETs and planar high frequency transformer.

1. INTRODUCTION
For on-board power electric applications (traction, or auxiliary unit power supply) a candidate and mature fuel cell generator is the PEMFC technology with proton exchange membrane electrolyte. In that case, to perform the traction function of an electric vehicle, it must be of sufficient power (in general several tens of kW). The power increase of fuel cells is achieved by long stacks of cells units (greater than one hundred) as well as by an increase of their active surface. Nevertheless, the increase of the number of cells is limited by mechanical constraints and waterproofness of cell units [1]. Moreover a large number of cells or a too wide active surface makes the fluidic management of the fuel cell difficult. In such a case, disparities in the reactant gas supply can appear within a cell [2, 3] or between them [4]. It results non-uniformity between the cell voltages and a possible appearance of defects like flooding or drying. Therefore, the use of several fuel cells stacks allows an increase of power while using standard-technology modules with easy design and management. This idea is called the "multi-stack association concept" and has already been presented in [5, 6]. Besides, a disparity of temperature throughout the stack makes that flooding mainly appears on the extremities of the stack, where the temperature is lower, whereas drying takes place rather in the center of the fuel cell where the temperature is higher [7-11]. Thus, during the appearance of a defect, which can only affect some cells, a corrective action must be taken on the whole stack including also the healthy cells. A fluidic action based on fuel cell conditioning auxiliaries (air compressor, humidifier, temperature regulation) is already a solution. However, for long stacks, faults can appear on localized areas, mainly affecting some cells or groups of cells [12, 13]. Consequently, the fluidic circuitry may become complex to be used in case of fault appearance. In this paper, electrical power conditioning is explored as a new corrective action. For this purpose, power converters can be considered either as a global electrical interface for the FC generator or can act on localized areas of the stack. Indeed, as fuel cell voltage significantly varies according to power, these converters are naturally present in a fuel cell system to regulate the load voltage. Considering the fact that faults will mainly affect some particular cells or groups of cells [12], localized power converter architecture will be rather investigated coupled to a 3-part segmented power fuel cell [6]. The associated modular architecture should be reliable and cost-effective and should have high energy efficiency such as not to penalize the nominal functioning of the fuel cell generator. The present paper is organized as follows. First (section 2) a fault detection

strategy for PEM fuel cell is exposed. Section 3 discusses the respective interests of the AC and the DC couplings for managing power between the fuel cell segments and the load. For the case of DC-link power transfer, the resonant isolated boost (R.I.B.) topology is revealed as an efficient candidate. Section 4 focuses on the multi-port electrical architecture control strategy and technology considerations in order to design the 30kW prototype converter.

2. FEEDBACK ON THE FAULT DETECTION STRATEGY

A fault detection strategy has been proposed by Frappé *et al.* in [12]. It basically relies on voltage measurement and intends to make use of the small disparity of temperature as well as the non-uniform distribution of reactants along the stack. Indeed, many authors pointed out the cell discrepancies throughout the stack which depend on the operating conditions [4]. Some authors observed that cell voltage is lower in the cells furthest from the fuel inlet of the stack (nearest to the air inlet) due to uneven gas distribution or water flooding [10, 11]. Different experiments also indicate that the central region of the stack is hotter than its exterior and subsequently drying mostly occurs in center cells [9, 10]. Indeed, Ramousse *et al.* [7] positively highlights that liquid water in the cells is highly dependent on the temperature; as a result flooding occurs in cooler cells and drying in hotter cells. Based on these remarks, we suggest measuring the voltage of group of cells in the inlet, the center and the outlet of the stack (Fig. 1). The methodology has been implemented and tested on a 20-cell 500W PEMFC set-up at FCLAB in Belfort, France [13].

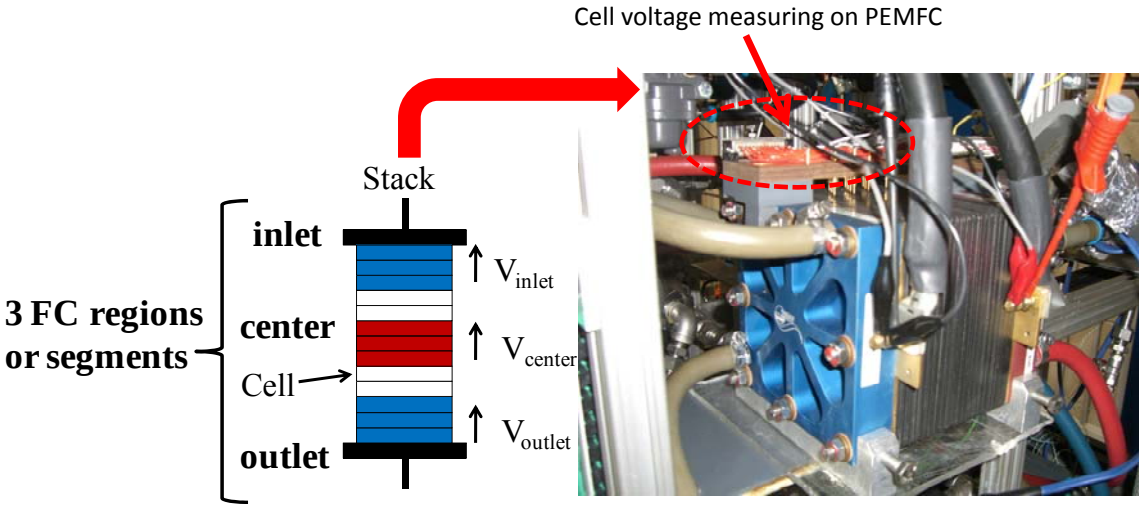

Figure 1. Fault detection strategy for PEMFC and experimental set-up

It appears relevant to instrument the FC with voltage sensors in three main areas of the stack: the inlet, the outlet and the center. In this case, the detection principle is based on the monitoring of a differential between the voltage in the center of the stack (Vcenter) and the inlet/outlet voltages (resp. Vinlet, Voutlet). This principle allows generating a new state-of-health indicator of the fuel cell stack. In the case of no fault, all voltages are constant or drop similarly due to load variation: the differential voltage equals zero. If a drying appears, only Vcenter drops and the two differential voltages become positive. Conversely, if a flooding occurs, the inlet and/or the outlet voltages drop leading to a decrease of one or two differential voltages. Using the differential method, the FC stack can be assimilated to a voltage sensor. Its characteristic is to provide two key signals representative of the state of health. The feedback information is simple, fast and based on the real-time operating conditions without adding any external disturbance. Moreover the method can be applied also when the operating conditions are slightly modified.

3. CONVERTER TOPOLOGY ANALYSIS FOR THE POWER TRANSFER

Power transfer between different fuel cell segments and the load can be achieved via two types of electrical links: one AC-link or a DC-link. AC-link authorizes directly the power transfer through the transformer, for example thanks to the use of a multi-windings transformer. DC-link imposes an indirect conversion but permits to regulate easily the power between the different segments thanks to

the DC node. Figs. 2a and 2b illustrate the principle of power transfer using AC and DC-link. Segmentation of the fuel cell imposes galvanic isolation between segments and the load.

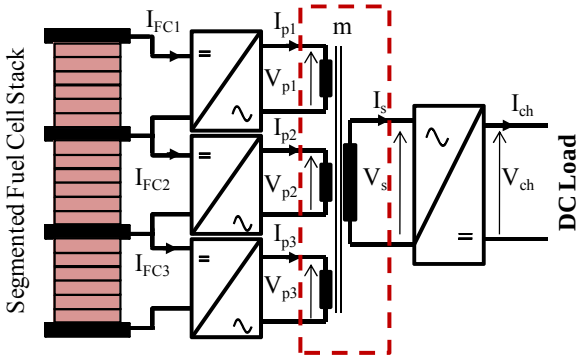

Figure 2a. Electrical architecture with AC-link

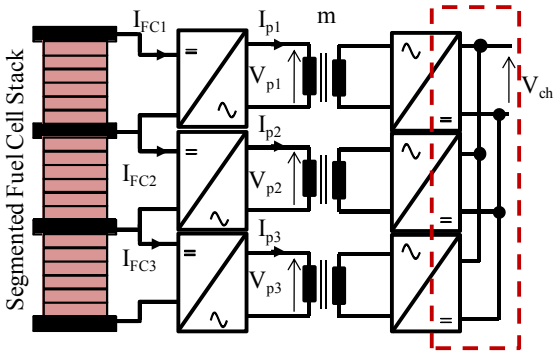

Figure 2b. Electrical architecture with DC-link

Technical specifications are as follows: The 30kW fuel cell generator is subdivided into 3 equal parts of 10kW, 200 cm2 of active area, 100 cells.

- No-load voltage: 100V
- Rated current: 166 A
- Rated Voltage: 60V

The power converter is able to regulate the output power to 540 VDC; this value is a standard in railways and heavy land vehicles. The following study is focused on one "converter brick" associated to one fuel cell segment.

3.1 Power transfer through the AC-link: the Phase-shifted inverter topology

The segmented concept for the fuel cell implies the use of insulation between the segments; a first approach concerns the possibility of using the AC-link for the power transfer. Some research works have already been published on the topic [14-18]. Each port of the transformer is connected to a voltage source inverter which delivers a rectangular shaped voltage (-V, 0, +V). The power transfer between two ports is achieved thanks to a voltage shift. The leakage inductance L_k and the switching frequency also interfere in the power transfer adjustment (Figs. 3a and 3b). This topology allows an effective regulation of the power between different ports.

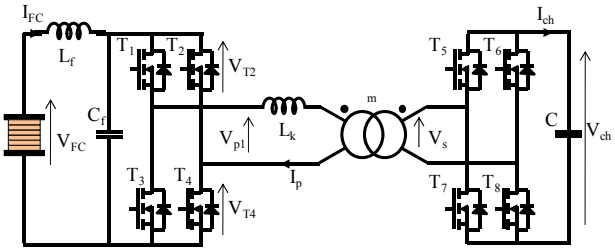

Figure 3a. Phase-shifted inverter topology for AC coupling

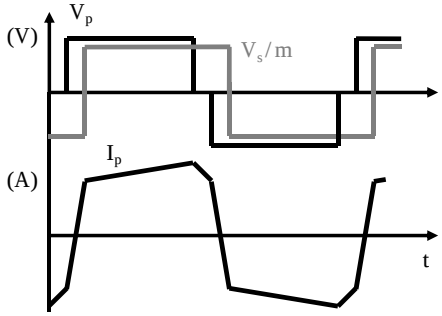

Figure 3b. Phase-shifted inverter: Typical waveforms

Moreover, Frappé *et al.* have proposed a control methodology which is able to decouple the energy fluxes issued from each converter. In order to achieve this properly, output AC voltage (V_s) and current (I_s) are set in phase. Furthermore, taking into account the proposed control strategy, a zero voltage switching (ZVS) mode is possible hence enabling switching losses reduction. This strategy has been proposed in [14]. However, the phase-shifted inverter topology is optimal only when the AC voltages V_p and V_s/m have the same amplitude: in the absence of phase-shift, no current circulates through the leakage inductance L_k permitting to perform no active power without reactive power. This topology is hence very sensitive to the FC input voltage variations. Any voltage fluctuation causes a

reactive current which can be significant within the AC link. Furthermore, because of the voltage inverter structure, the inverter input current presents a large AC component which can induce negative impact on the fuel cell. As a consequence adding an input filter is mandatory, but leads to increase the size of the converter. Hence, the use of the AC-link is not recommended namely because of the constraints impacting the fuel cell characteristics. For this reason, another type of electrical coupling is considered: the DC-link coupling.

3.2 Power transfer through the DC-link: the Resonant Isolated Boost (R.I.B.) as a candidate

Isolated DC/DC conversion structures have been considered for the power transfer through the DC-Link. Half-Bridge and Full Bridge isolated boost have been the first explored topologies [19, 20]. However, these two isolated boost topologies operating on hard-switching mode require a clamping circuit during the transistor switch-off because of the influence of transformer leakage inductance. This clamping circuit can be either active by the addition of a capacity and a switch [21] or passive by the addition of a diode, a capacity and a resistance [23]. For both cases, the losses of the converter are increased. Another possibility is to make the MOSFETs operate in avalanche mode; the resulting avalanche energy is then transferred into the switches and no additional clamping element is required [22]. In order to use the MOSFETs in avalanche, it is necessary to make sure that the leakage inductance L_k of the transformer is the smallest possible and the sizing of heat sink should take into account this constraint. Hence, to make sure to minimize at most the losses of the converter, a third topology, based on resonance, is explored, enabling high frequency operation and soft switching.

This resonant topology is the resonant isolated boost (R.I.B.) cited by [23-26] and presented in Fig. 4a. A capacitor C_p is added to establish a quasi-resonant circuit with the leakage inductance L_k. Hence, this structure is not subject to voltage peaks due to the opening (switch-off) of semiconductor switches. The resonant circuit allows obtaining an operation at zero current switching (ZCS) (Fig. 4b). The converter control is now realized by frequency tuning. In steady-state, the load voltage vs. fuel cell voltage relation is given by equation (1):

$$V_{ch} = \frac{m}{1-\frac{f}{f_r}} V_{FC} \qquad (1)$$

This equation demonstrates that the converter frequency control significantly evolves according to FC voltage variation. Namely, considering a fixed output voltage (V_{ch}) and a [VFC / 2; VFC] fuel cell voltage range, the control frequency varies from f_{min} to f_{max} = 2.5 f_{min}. Moreover, over the whole converter working range, the ZCS mode has to be validated. The converter operating frequency is chosen between 17 kHz and 38 kHz; f_{max} corresponds to the maximal current. These frequency values are a trade-off between acceptable semiconductors losses and size of the high frequency transformer. Resonant circuit parameters are L_k = 1.62µH and C_p= 2.61µF.

$f_r = \frac{1}{2\pi\sqrt{L_k C_p}}$ = 78 kHz is the resonant frequency. Selecting a transformer ratio m= 4, an inductance L= 38µH, the constraints on the semiconductor switches are computed as follows:

$$V_{T\,max} = \frac{V_{ch}}{m} = 135V \qquad I_{T\,max} = \frac{V_s}{m\sqrt{\frac{L_k}{C_p}}} = 170A \qquad V_D = V_{ch} = 540V \qquad I_{D\,max} = \frac{I_{FC}}{m} = 40A$$

Fig. 4a shows the fuel cell power according to converter frequency. The rated power (10 kW) is achieved for the maximal frequency of 38 kHz. Moreover, ZCS mode is achieved (Fig. 4c), which leads to a significant reduction of the dynamic losses.
The FC current ripple ΔI_{FC} can be computed as (2):

$$\Delta I_{FC} = \left(\frac{m I_{FC} L_k}{V_{ch}} + \frac{1}{2\pi f_r} \cdot \left(\pi - a\sin\left(\frac{m I_{FC} Z_r}{V_{ch}} \right) \right) \right) \cdot \frac{V_{FC}}{L} \qquad (2)$$

For a current ripple equal to 10% of I_{max} (maximal current = 160A), the input inductance value is L= 38 µH. Hence for IFC=122A, ΔIFC= 12.5A, and for IFC=32A, ΔIFC= 14A. Fig. 4d illustrates the fuel cell current ripple according to FC voltage and FC current in a 3D-axis view. The FC ripple is slightly impacted (16A at no-load to 10A at full load) over the global FC operating range.

Figure 4. Resonant isolated boost characteristics applied for one PEMFC segment of 10kW

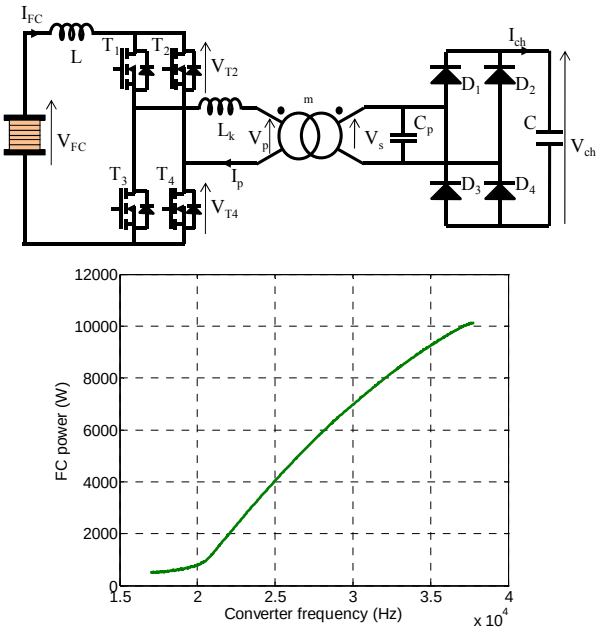

Figure 4a. R.I.B. with FC power vs. frequency

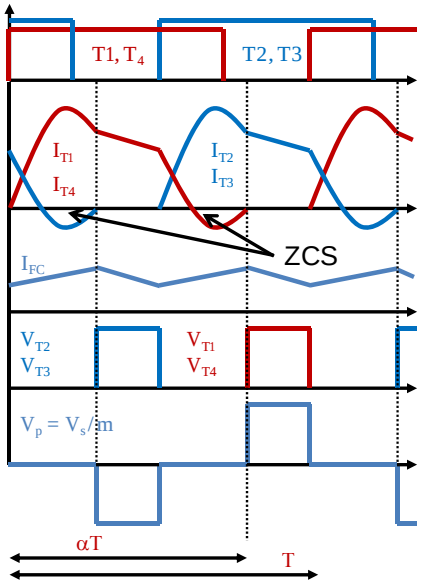

Figure 4b. R.I.B. typical waveforms

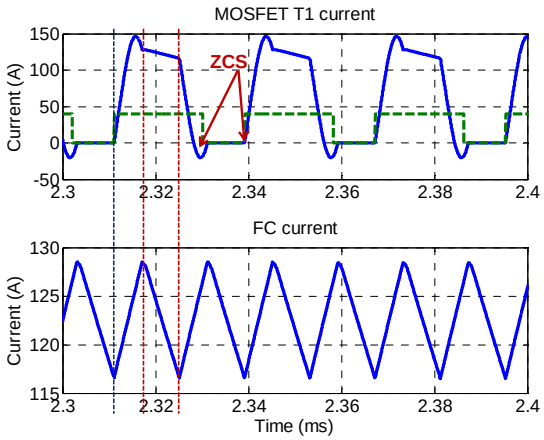

Figure 4c. MOSFET T1 current and FC current ripple for 122A test

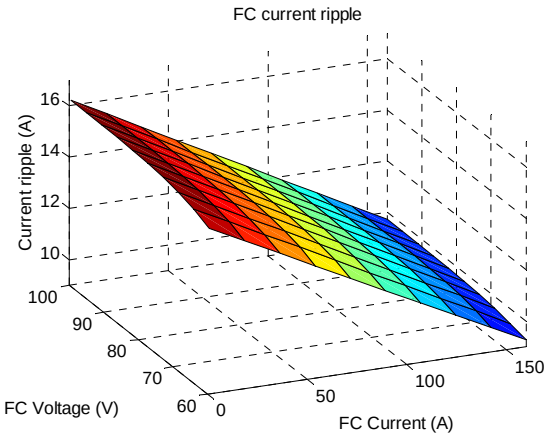

Figure 4d. FC current ripple in a 3D-axis view

4. MULTI-PORT ELECTRICAL ARCHITECTURE CONTROL STRATEGY AND TECHNOLOGY CONSIDERATIONS

4.1 Control strategy of the 30kW multi-port PEMFC system and degraded modes management

The resonant isolated boost has been adopted in order to realize the converter system associated to the 3-part segmented PEM fuel cell. Output voltage regulation of the 3-part segmented PEM fuel cell is performed using two cascaded loops and the principle shown in Fig. 5. The outer loop is common to all the system and aims at regulating the bus voltage. The current reference Iref calculated by this regulation is sent to a current dispatcher. This dispatcher distributes each converter current set point according to the global value Iref and the state of health of each segment. The three inner loops

compare the current reference values with measured current values (I_{FC1}, I_{FC2}, I_{FC3}) and hence define each converter frequency control value (f_ref1, f_ref2, f_ref3). As a result, in nominal conditions, each converter current reference is equilibrated to a third of the global reference given by the voltage loop. On the contrary, while a failure affects one FC segment, a current split strategy is implemented in order to relieve the FC segment under fault. To be precise, the supervisor's role is to manage the current distribution (current split strategy) between FC parts according to the FC segments state-of-health. Moreover, in case of failure, and as a complement to the electric action, the supervisor has also the ability to modify the parameters of the fluidic auxiliaries. The load current may be also limited. Indeed, in case of sudden FC power decrease, it is mandatory to limit the DC load current in order to avoid a breakdown of the DC voltage.

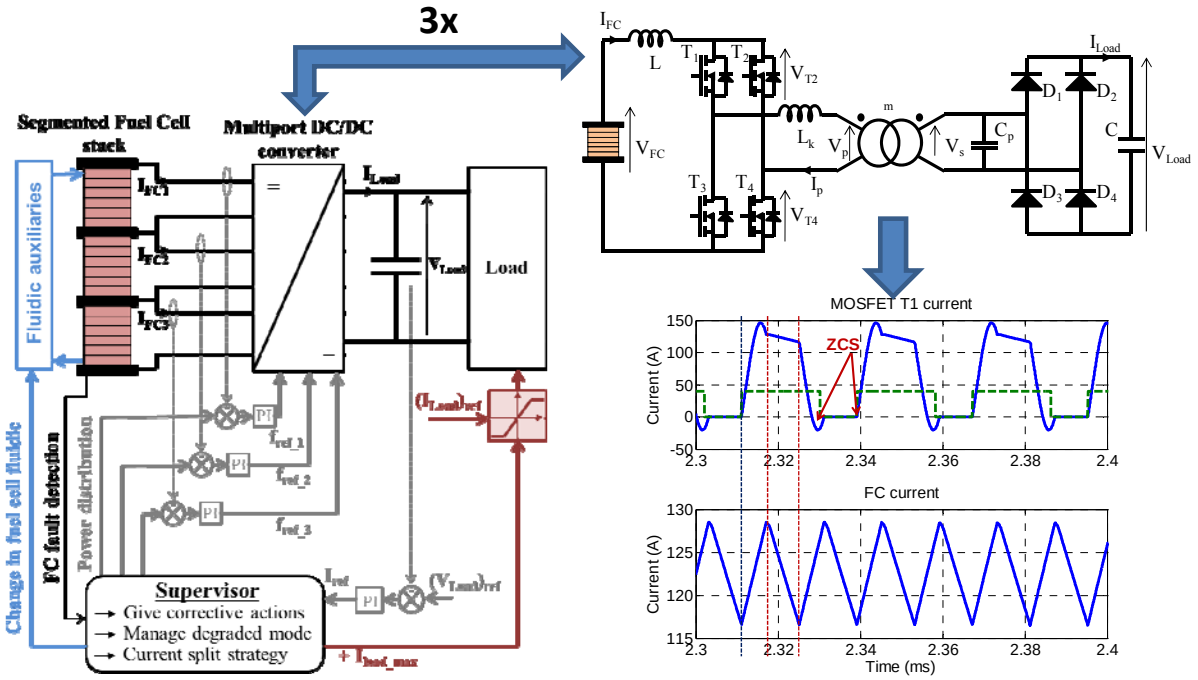

Figure 5. Synoptic of the 30kW multi-port system regulation strategy

The sample hypothesis is that the FC stack is under fault (unhealthy state), and one segment is affected by the fault. Two different tests using electric action rather than exploiting fluidic ancillaries' control are performed and illustrated by simulation using Matlab-Simulink®. The first one (noted Action 1) is a limited (or moderated) power action on one FC segment (partial segment power removing). The management strategy induces a current split of 2/3; 7/6; 7/6 for the 3 FC segments and with corresponding load limitation. The second action (Action 2) deals with a loss of an entire FC segment due to current cancellation (complete segment power removing). These simulations were discussed in [6], and key results summarized in this paper.

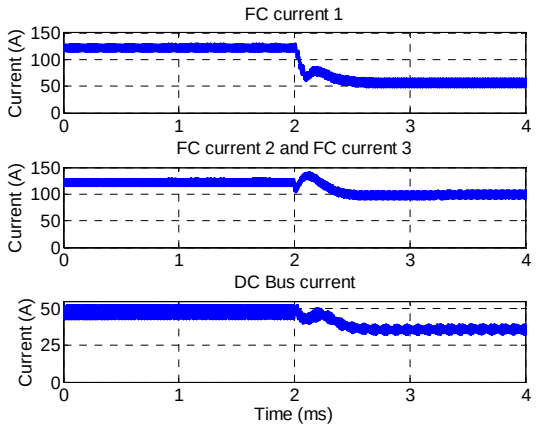

Figure 6a. Action 1: Moderated power correction

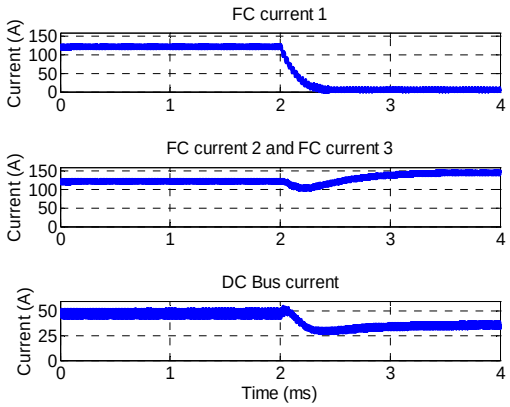

Figure 6b. Action 2: Complete segment

removing

4.2 Technology for the 30kW multi-port converter prototype

The implementation of a resonant isolated boost converter prototype requires specific technological choices. The design is done for one 10kW converter prototype, which represents the converter technology brick. High frequencies use (between 17 to 38 kHz) enables to use a planar transformer technology, which leads to a compact solution. The transformer is designed by Payton Company [27] with the desired characteristics: power 10kW, primary/secondary voltage 135/540V, primary/secondary current of 170/40A and a leakage inductance equal to 1.6 µH. As the primary transformer voltage is low (135V), and since high frequency range is aimed, MOSFETs technology is the best candidate for semiconductors. The chosen technology for the MOSFETs is the GigaMOS^{TM} IXFN230N20T (200V/220A) from IXYS [28]. It features low on-state resistance (Rdson = 7.5 mΩ at Tj=25°C), fast intrinsic diode, isolation voltage up to 2500 VAC, and standard package in compact SOT-227 module. Selected capacitances are medium power film capacitors from AVX, especially chosen for DC filtering. Finally, the input inductance design value is 38 µH while its rated current is 160A. It has to stand a 10% current ripple. For inductance coil technology, ferrite or iron powder cores are preferred. The converter is water cooled on a heat-sink plate.

Table 1. Technology for resonant isolated boost converter.

	Constraints (devices calibre)	**Technological choice**
Input inductance : L	38µH 160A ΔI=10% (+/-16A_{max})	Iron powder cores
MOSFETs : T_1 to T_4	135V – 170A	IXYS GigaMOS^{TM} IXFN230N20T (200V-220A)
HF Transformer	135 – 540V / 170 – 40A m = 4 10kW	Planar technology transformer from "Payton planar Magnetics"
Resonant capacitor : C_p	2.61µF 540V – 40A_{max}	4 capacitors in series from TPC-AVX FFV36C0136K (150Vrms – 25A_{rms})
Rectifier diode bridge : D_1 to D_4	540V – 40A	IXYS diodes DSEP2x91-06A (600V – 90A)
DC bus capacitor : C	50µF 540V – 20A	FFG86K0586K – 600V – 44A – 56µF

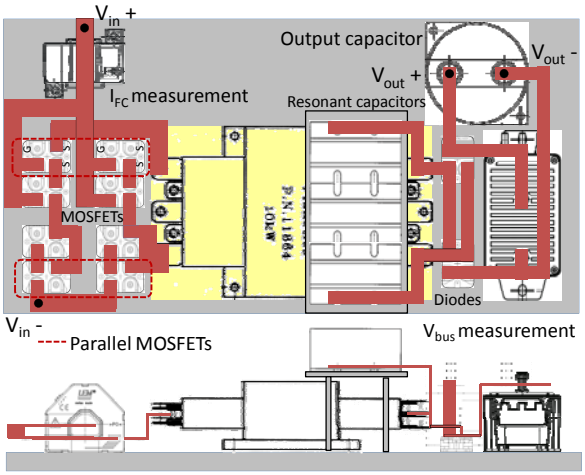

Figure 7a. 10 kW pre-prototype design technology implementation of the converter on heat sink

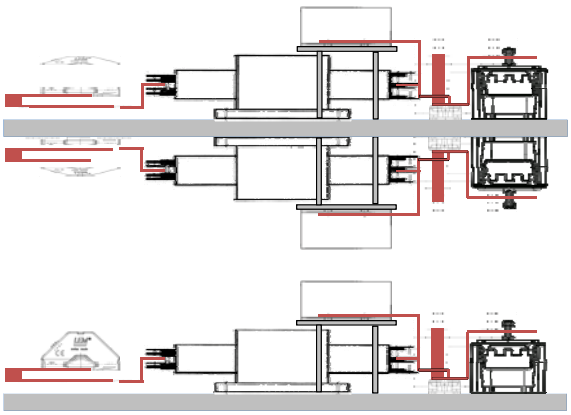

Figure 7b. Full 30kW converter implementation (symmetrical design over 2 heat-sinks)

The drivers will adapt the gate control signals to the MOSFETs. They offer a galvanic insulation and permit to deliver high current peaks. Dual-channel high-power SCALE-2 2SC0435T© Driver Core

from CT-Concept Technologie [29] have been selected in order to drive the MOSFETs. Fig. 7a presents the integration of the 10kW pre-prototype resonant isolated boost converter (semiconductors, diodes, HF planar transformer) on a water cooled heat-sink from AAVID THERMALLOY, with HF voltage, current sensors, and copper busbar connections. Fig. 7b illustrates the design symmetrical implementation of the full 30kW / 3-level converter on two separate heat-sinks.

5. CONCLUSION

Power PEM fuel cell stacks used for vehicle propulsion or on-board auxiliaries can be either made of long and single stacks, or composed of multiple fuel cell modules building a "multi-stack" association. Besides, the segmented concept for fuel cells gathers both compactness of a single fuel cell and the potentialities of "modularity" of a "multi-stack" system. However, this concept doesn't allow acting independently on the fluidic of each segment. In this paper, we suggest to compensate this drawback by an electric action through the converter. The present article points out that PEM fuel cell can be split into several segments both for failure detection and for relevant energy management. Fulfilling these objectives, the appropriate power architecture is based on a DC-link and ZCS isolated boost converters. The fuel cell health supervisor can act easily on the control board and hence drive the suitable power to each fuel cell segment. In our case a 30 kW PEMFC multi-port segmented system has been investigated and a pre-prototype converter has been proposed. Technology choices remain also important in order to ensure a compact high power density integrated power converter structure with improved efficiency and compatible with on-board requirements.

REFERENCES

1. P. Lin, P. Zhou, and C. W. Wu, "A high efficient assembly technique for large PEMFC stacks," *Journal of Power Sources*, vol. 194, no. 1: pp. 381-390, Oct. 2009.
2. S. G. Kandlikar, Z. Lu, T. Y. Lin, D. Cooke, and M. Daino, "Uneven gas diffusion layer intrusion in gas channel arrays of proton exchange membrane fuel cell and its effects on flow distribution," *Journal of Power Sources*, vol. 194, no. 1: pp. 328-337, Oct. 2009.
3. S. G. Kandlikar, Z. Lu, W. E. Domigan, a D. White, and M. W. Benedict, "Measurement of flow maldistribution in parallel channels and its application to ex-situ and in-situ experiments in PEMFC water management studies," *International Journal of Heat and Mass Transfer*, vol. 52, no. 7-8: pp. 1741-1752, Mar. 2009.
4. M. Miller and A. Bazylak, "A review of polymer electrolyte membrane fuel cell stack testing," *J. Power Sources*, vol. 196, no. 2, pp. 601-613, Jan. 2011.
5. A. De Bernardinis, M.-C. Péra, J. Garnier, D. Hissel, G. Coquery, and J.-M. Kauffmann, "Fuel cells multi-stack power architectures and experimental validation of 1kW parallel twin stack PEFC generator based on high frequency magnetic coupling dedicated to on board power unit," *Energy Conversion and Management*, vol. 49, no. 8: pp. 2367-2383, 2008.
6. A. De Bernardinis, E. Frappé, O. Béthoux, C. Marchand and G. Coquery, "Multi-port power converter for segmented PEM fuel cell in transport application. Simulation with fault-tolerant strategy" *Eur. Phys. J. Appl. Phys.* (2012) 58: 20901.
7. J. Ramousse, K.P. Adzakpa, Y. Dubé, K. Agbossou, M. Fournier, A. Poulin, and M. Dostie, "Local Voltage Degradations (Drying and Flooding) Analysis Through 3D Stack Thermal Modeling," *J. Fuel Cell Science and Technology*, vol. 7: 2010, p. 041006.
8. A. Hernandez, R. Outbib, and D. Hissel, "Diagnostic d'une pile à combustible PEMFC. Une approche statistique," *Journal Européen des Systèmes Automatisés*, vol. 42, no. 10: pp. 1225-1277, 2008.
9. J. Jang, H. Chiu, W. Yan, and W. Sun, "Effects of operating conditions on the performances of individual cell and stack of PEM fuel cell," *J. Power Sources*, vol. 180, no. 1: pp. 476-483, May 2008.
10. R. Eckl, W. Zehtner, C. Leu, and U. Wagner, "Experimental analysis of water management in a self-humidifying polymer electrolyte fuel cell stack," *J. Power Sources*, vol. 138, no: 1-2 pp. 137-144, Nov. 2004.

11. W. H. Zhu, R. U. Payne, D. R. Cahela, and B. J. Tatarchuk, “Uniformity analysis at MEA and stack Levels for a Nexa PEM fuel cell system,” *Journal of Power Sources*, vol. 128, no. 2, pp. 231-238, Apr. 2004.
12. E. Frappé, A. De Bernardinis, O. Bethoux, D. Candusso, F. Harel, C. Marchand and G. Coquery, “PEM fuel cell fault detection and identification using differential method: simulation and experimental validation,” *Eur. Phys. J. Appl. Phys.* 54: 23412 (2011).
13. E. Frappé, A. De Bernardinis, O. Bethoux, D. Candusso, F. Harel, C. Marchand and G. Coquery, "Fault detection by localized voltage measurement on a PEMFC stack", in Fundamentals and Developments of Fuel Cells Conference (FDFC 2011), 19-21 January 2011, Grenoble.
14. E. Frappé, A. De Bernardinis, O. Bethoux, C. Marchand, and G. Coquery, “A Soft-Switching Multisource DC-DC Converter for Segmented PEM Fuel Cell Power Management in Vehicle Application,” in Proc. IEEE Vehicle Power and Propulsion Conference, Chicago, September 2011.
15. S. Mariethoz and A. Rufer, “Multisource DC-DC converter for the supply of hybrid multilevel converter,” Conference Record of the 2006 IEEE Industry Applications Conference Forty-First IAS Annual Meeting, vol. 2, no. c, pp. 982-987, Oct. 2006.
16. N. Schibli, “DC-DC converters for two-quadrant operation with controlled output voltage,” in Proc. EPE 99, Lausanne, September 1999, pp. 1-7.
17. F. Krismer, S. Round, and J. Kolar, “Performance optimization of a high current dual active bridge with a wide operating voltage range,” in Proc. Power Electronics Specialists Conference, PESC’06. 37th IEEE, 2006, vol. pp, pp. 1–7.
18. C. Zhao, S. D. Round, and J. W. Kolar, “An isolated three-port bidirectional DC-DC converter with decoupled power flow management,” Power Electronics, IEEE Transactions on, vol. 23, no. 5, pp. 2443–2453, Sep. 2008.
19. Y. Lembeye, V. D. Bang, G. Lefevre, and J.-P. Ferrieux, “Novel Half-Bridge Inductive DC–DC Isolated Converters for Fuel Cell Applications,” *IEEE Trans. on Energy Conversion*, vol. 24, no. 1: pp. 203-210, Mar. 2009.
20. M. Nymand and M. A. E. Andersen, “High-Efficiency Isolated Boost DC–DC Converter for High-Power Low-Voltage Fuel-Cell Applications,” *IEEE Trans. on Industrial Electronics*, vol. 57, no. 2: pp. 505-514, Feb. 2010.
21. A. Vazquez, C. Aguilar, and F. Canales, “Comparison between two-stage and integrated power conditioner architecture for fuel cell based power supply system,” in Power Electronics Congress, 2008, CIEP 2008. 11th IEEE International, 2008, pp. 177–184.
22. K. Wang, C. Y. Lin, L. Zhu, D. Qu, F. C. Lee, and J. S. Lai, “Bi-directional DC to DC converters for fuel cell systems,” in Power Electronics in Transportation, 1998, 1998, pp. 47–51.
23. H. Benqassmi, J.-P. Ferrieux, and J. Barbaroux, “Current-source resonant converter in power factor correction,” in Proc. PESC97. Record 28th Annual IEEE Power Electronics Specialists Conference, 1997, pp. 378-384.
24. J.-F. Chen, R.-Y. Chen, and T.-J. Liang, “Study and Implementation of a Single-Stage Current-Fed Boost PFC Converter With ZCS for High Voltage Applications,” *IEEE Trans. on Power Electronics*, vol. 23, no. 1, pp. 379-386, Jan. 2008.
25. R. Y. Chen, R. L. Lin, T. J. Liang, J. F. Chen, and K. C. Tseng, “Current-fed full-bridge boost converter with zero current switching for high voltage applications,” Fourtieth IAS Annual Meeting. Conference Record of the 2005 Industry Applications Conference, 2005, pp. 2000-2006, 2005.
26. R.-Y. Chen, T.-J. Liang, J.-F. Chen, R.-L. Lin, and K.-C. Tseng, “Study and Implementation of a Current-Fed Full-Bridge Boost DC–DC Converter With Zero-Current Switching for High-Voltage Applications,” *IEEE Trans. on Industry Applications*, vol. 44, no. 4, pp. 1218-1226, 2008.
27. P. Špánik, I. Feňo, G. Kácsor, I. Lokšeninec, “Using planar transformers in soft-switchng DC-DC power converters”, Application Note, consulted online 5 March 2013 at: http://www.paytongroup.com/info/Planar trans._paper.pdf.
28. Tech. Datasheet IXFN230N20T, IXYS Corp. 2011, http://www.ixys.com/
29. Driver SCALE-2 Concept datasheet, http://www.igbt-driver.com/produtcs/scale-2/scale-2-cores/2sc0435t.html (consulted online 5 March 2013).